INTL JOURNAL OF ELECTRONICS AND TELECOMMUNICATIONS, 2023, VOL. 69, NO. 3, PP. 431-437
Manuscript received January 2, 2023; revised July, 2023. DOI: 10.24425/ijet.2023.144380

A Compact Quasi-Yagi Microstrip Patch Antenna with High Gain and Bandwidth for UWB Application

Hasanur Rahman Chowdhury, and Sakhawat Hussain

***Abstract*—A quasi-Yagi microstrip patch antenna with four directors and truncated ground plane has been designed and fabricated to have an ultra-wide bandwidth, high gain, low return loss and better directivity with center frequency at 3.40 GHz. After optimization, the proposed antenna yields an ultra-wide bandwidth of 1.20 GHz with lower and upper cutoff frequencies at 3.12 GHz and 4.32 GHz, respectively. High gain of 5.25 dB, return loss of -28 dB and directivity of 6.28 dB are obtained at resonance frequency of 3.40 GHz. The measured results of fabricated antenna have shown excellent agreement with the simulation results providing bandwidth of 1.34 GHz with lower and upper cutoff frequencies at 3.04 GHz and 4.38 GHz, respectively. The antenna gain of 5.33 dB, return loss of -44 dB are obtained at resonance frequency of 3.36 GHz. The dimension of the antenna is only of 65 mm x 45 mm ensuring compact in size.**

***Keywords*—Quasi Yagi microstrip patch antenna; FR4 substrate; ultra-wide bandwidth (UWB); high antenna gain and low return loss**

I. INTRODUCTION

IN wireless communication, an antenna plays a vital role in deciding the quality and overall performance of the device over different communication standard. Since the inception of Yagi-Uda antenna[1],[2], huge research effort has been devoted to modify it (known as quasi-Yagi Uda antenna) to overcome its limitations, such as relatively large size, narrow band (<5%) characteristics and tuning difficulties. As a part of that process, an antenna structure with microstrip radiator technique and Yagi-Uda array concept was first introduced by Huang et al [3]. Later, Qian et al proposed the printed microstrip patch antenna for wireless communication [4]. After the Federal Communications Commission (FCC) of the United States adopted the First Report and Order that permit to use the Ultra Wide Band (UWB) technology for commercial operation and allocated a bandwidth of 7.5 GHz from 3.1 GHz to 10.6 GHz for unlicensed use, huge research have been carried out to develop and implement UWB antennas [5] . Researchers tried to develop different shape such as fork [6], elliptical [7], square [8], octagon [9], top-hat monopole [10], bowtie active elements [11], slot Yagi like multilayered [12] microsrtip antennas and so on, for UWB application.

Different transition such as coplanar waveguide (CPW) to coplanar strip (CPS) [13], uniplanar microstrip-to-CPS[14], compact planar microstrip-fed [15], CPW-fed [16] and CPS-fed [17] Yagi antenna have been reported. Yet, all these antennas have one or other limitations like narrow bandwidth, larger size, less directivity, low gain, antenna complexity or manufacturing difficulties and so on. Hence, search for a perfect design and easy to construct quasi- Yagi antenna with good radiation pattern behavior is still on.

This research work aims to develop a quasi-Yagi antenna with balance and unbalance (balun) section, made up of microstrip to CPS transition section, to match the feed-line impedance, truncated ground plane as reflector and several directors. It is to achieve relatively low return loss, high gain, high directivity and compact size antenna operating at center frequency of 3.4 GHz with a bandwidth covering the ultra-wideband (UWB) range. This antenna could be used in such locations where not omni-directional rather some directional radiation coverage are required for UWB applications. Firstly, the quasi-Yagi antenna is designed and optimized using the software platform known as Computer Simulation Technology (CST) studio, a highly used software that provides accurate and efficient computational solutions for electromagnetic design and analysis. Afterwards, the design parameter of the antenna are implemented on FR4 substrate with dielectric constant (ε_r) of 4.3 and thickness (H_s) of 1.5 mm. It has copper cladding on both sides of thickness (h_t) 0.035 mm. The choice of FR4 epoxy substrate other than PTFE-based substrate like Rogers or RT/duroid is due to its low cost and excellent mechanical properties for various electronic component applications [18]. The fabricated antenna was then tested using a Vector Network Analyzer (Rohde and Schwarz-ZVH8) and Wave, and Antenna Training System (Man and TEL Co.).

II. DESIGN PROCEDURE OF THE PROPOSED QUASI-YAGI ANTENNA AT 3.40 GHZ

The schematic diagram of top view of the proposed quasi-Yagi antenna along with its different parts and their dimension notation are shown in Fig. 1. Since the targeted resonating frequency (f_c) is at 3.40 GHz and the dielectric constant of the substrate is (ε_r) of 4.3, so the free space wavelength is

This wrok was partially funded by the Higher Education Quality Enhancement Program (HEQEP) of the University Grants Commission of Bangladesh.

Hasanur Rahman Chowdhury is with 1) Department of Electrical and Electronic Engineering, University of Dhaka, Dhaka-1000, Bangladesh; 2) Department of Electrical & Computer Engineering, Michigan State University, East Lansing, Michigan, USA (e-mail: hasanrchowdhury@gmail.com).

Sakhawat Hussain is with the Department of Electrical and Electronic Engineering, University of Dhaka, Dhaka-1000, Bangladesh (e-mail: sakhawat@du.ac.bd - corresponding author).

calculated as $\lambda_0 = \frac{c}{f_c} = 88.24\,mm$; whereas the guided wavelength within the antenna will be $\lambda_g = \lambda_0/\sqrt{\varepsilon_r} =$ 42.55 mm. The individual section of the proposed quasi-Yagi antenna along with their parameter values are described in the following sub-sections.

A. Microstrip Feedline parameters:

Assuming that the microstrip feedline width (W_f) is larger than the substrate thickness (H_s), the effective dielectric constant (ε_{eff}), microstrip feedline width (W_f) and input impedance (Z_0) of the system can be expressed as follows [19]:

$$\varepsilon_{eff} = \frac{\varepsilon_r+1}{2} + \left[\frac{\varepsilon_r-1}{2\sqrt{1+12\left(\frac{H}{W}\right)}}\right] \quad (1)$$

$$W = \frac{V_0}{2\times f_r} \times \sqrt{\frac{2}{\varepsilon_r+1}} \quad (2)$$

$$Z_0 = \frac{120\pi}{\sqrt{\varepsilon_{eff}}\left[\frac{W}{H}+1.393+\frac{2}{3}\ln\left(\frac{W}{H}+1.444\right)\right]} \quad (3)$$

By following equation 1 to 3 to match the input impedance Z_0 = 50 Ω, the feedline width is calculated as W_f = 2.87 mm. However, the direct calculation of feedline width (W) from equation 2, where V_0 is the speed of light in free space, gives the value to be of 27.1 mm. As the microstrip feedline width (W_f) value may varies from $\frac{W}{5}$ to $\frac{W}{15}$ to that of theoretically calculated value (W) to match the input impedance value, here we considered the feed line width to be of 2.87 mm in our simulation work. The length of the feedline (L_f) is not that crucial to match the impedance, so it is set as of 7.5 mm (less than quarter wavelength $\frac{\lambda_g}{4} \approx 10.6\,mm$) by optimizing in CST studio.

B. Microstrip to coplanar strip (CPS) transition section

This section construct a balance to unbalanced (Balun) part by employing a quarter-wave long transformer, a symmetric center V grooved T-junction power splitter and Miters for the 90° microstrip bends. As shown in Fig. 1(a) that the right arm and the left arm of the T-junction power splitter also act as a quarter-wave long transformer in our proposed antenna. For a lossless (reflection coefficient, $\Gamma = 0$) system the impedance of the T-junction arms should be such that it obey the following relation[19]:

$$Z_{IN} = \sqrt{Z_0.R_L} \quad (4)$$

Where the Z_{IN} is the characteristic impedance of the quarter wave transformer, Z_0 is input impedance of the T-junction and the R_L as load impedance from the quarter wave section. Since an equal power split is desired (-3db) for each arm and considering the arm impedance of 50Ω then the input impedance of the T-junction should be 25Ω and the characteristic impedance of the quarter wave transformer will be from equation 4, $Z_{IN} = \sqrt{Z_0.R_L} = 35.35\,\Omega$.

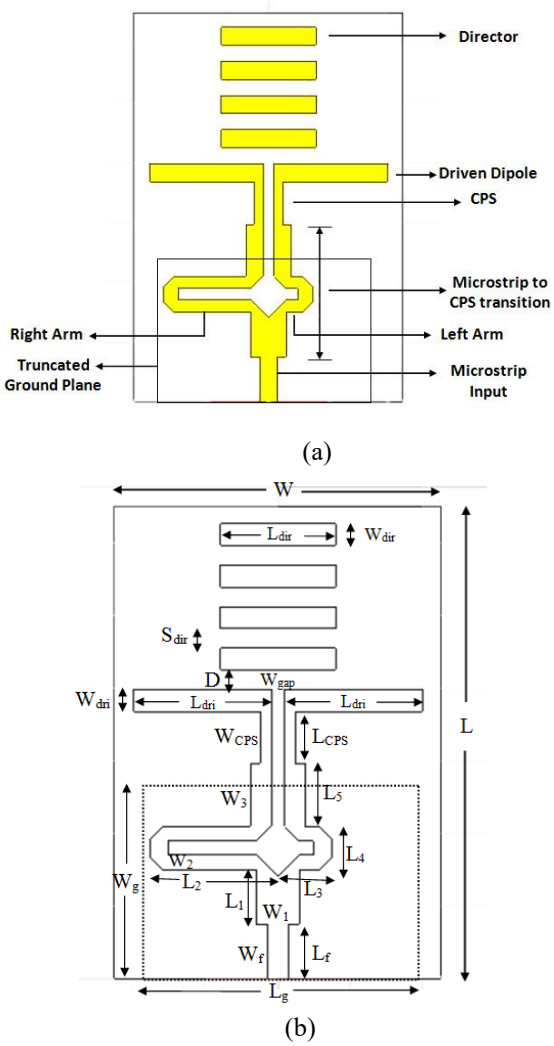

Fig. 1. Schematic diagram of proposed antenna along with (a) different parts and (b) their dimension notation

Moreover, to compensate the 180° phase delay introduced by the T-junction, the right arm length (L_2) is taken to be 17.6 mm and the left arm length (L_3) is 7.4 mm. These values are considered such to keep the path length distance of the two arms as $L_2 - L_3 = 10.4\,mm \approx {}^{\lambda_g}/_4$ so that an odd mode coupling is created between the two arms of the balun to provide the broadband characteristics of the antenna. Moreover, miters for the 90° microstrip bends at the corners of the T-junction has been introduced to reduce some capacitance and restores the original characteristic impedance. For a microstrip line of width W and height H, the diagonal D of the 'Square' shaped miter can be calculated from some empirical equations for designing a meter bend as [20]:

$$D = \sqrt{2} \times W \quad (5)$$

$$X = D \times [0.52 + 0.65e^{-1.35*\left(\frac{W}{H}\right)}] \quad (6)$$

$$A = \left(X - \frac{D}{2}\right) \times \sqrt{2} \quad (7)$$

While the conditions: $0.5 \leq \left(\frac{W}{H}\right) \leq 2.75$ and $2.5 \leq \varepsilon_r \leq 25$ are fulfilled. The dimensions D, X and A of the meter bend are shown in Fig. 2.

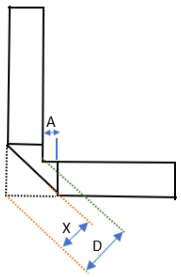

Fig. 2. Square shaped meter bends

In our design, we have considered the width (W) of the meter bend to be 2 mm, thus the diagonal dimension (D) become $2\sqrt{2}$ mm and $X = 1.77$ mm and $A = 0.5$ mm.

C. Co-planar strip line (CPS) section

The broadband balun's two arms are associated with a pair of coplanar striplines separated by a certain gap width (W_{gap}). These CPS lines direct the signal toward the end-fire radiation through the directors. CPS lines are first connected to the microstrip transition lines whose width (W_3) value is that of feedline width $(W_f = 2.87\ mm)$, length (L_5) is 8.6 mm and gap width (W_{gap}) of 1.778 mm. These transition lines serve as impedance matching lines to that of CPS lines. The CPS lines are shorter and narrower than the transition lines to compensate for the second-order discontinuities. The length and width of CPS lines are of (L_{CPS}) 7.196 mm and (W_{CPS}) 1.5 mm, respectively. The length and width of transition line and CPS sections are set by optimizing the design using software simulation.

D. Driver, directors and reflector sections

In a classic Yagi antenna the length of the driver element is $\frac{\lambda_g}{2}$. However, in our design, we have used dipole driver of length (L_{dri}) 19 mm, which is close to $\frac{\lambda_g}{4}$ and the width $(\mathrm{W_{dri}})$ is taken as 3mm, approximately that of feedline width $(\mathrm{W_f})$. The directors act as a guiding part of the antenna that ensures the end-fire radiation. The number and length of each director generally increase antenna gain and bandwidth. Nevertheless, it also makes the antenna size bulky. Considering compact size, in our design we have chosen four directors of equal length ($\mathrm{L_{dir}}$) of 15.9 mm (<$\mathrm{L_{dri}}$) by optimizing its value. The width of the directors are kept the same as driver width ($\mathrm{W_{dri}} = \mathrm{W_{dir}}$). The separation between each director are optimized at 2.7 mm. Finally, in a microstrip quasi-Yagi antenna, the ground plane serves as the reflector. Usually, the ground plane is truncated along one direction to make the antenna size small with higher gain and better directivity than a usual microstrip antenna [21], [22]. In this work, both the lateral and longitudinal lengths are truncated. After several trials, the reflector's length (L_g) and width (W_g) optimum values are set as 36.2 mm and 23.9 mm, respectively.

To accommodate all these above mention parts of the proposed quasi-Yagi antenna the total substrate size of the antenna has been optimized to be $65\ mm \times 45\ mm$ $(0.73\ \lambda_0 \times 0.5\ \lambda_0)$. The summary of all the optimized antenna parameters are listed in Table I.

III. RESULTS AND DISCUSSION

After optimization of all the antenna parameters using CST studio, we have constructed the proposed antenna using standard fabrication technique. Figure 3 shows the top and backside view of the fabricated antenna. The key features of the antenna such as return loss (S_{11}), voltage standing wave ratio (VSWR), gain, directivity, and radiation pattern have been evaluated using Vector Network Analyzer (VNA) and Wave and Antenna Training System of our lab.

TABLE I
OPTIMIZED PARAMETERS FOR THE STRUCTURE

Parameter	Antenna Element	Length (in mm)
W	Width of Substrate	45
L	Length of Substrate	65
W_g	Width of Ground Plane	23.9
L_g	Length of Ground Plane	36.2
W_f	Width of Feed Line	2.87
L_f	Length of Feed Line	7.5
W_1	Width of Transformer	6
L_1	Length of Transformer	7.5
L_2	Length of Right Arm	17.6
L_3	Length of Left Arm	7.4
L_4	Length of T-Junction	6
W_2	Width of T-Junction	2
L_5	Length of T-Junction to CPS	8.6
W_3	Width of T-Junction to CPS Transition Line	2.87 (W_f)
L_{CPS}	Length of CPS	7.196
W_{CPS}	Width of CPS	1.5
W_{gap}	Separation between both CPS	1.778
L_{dri}	Length of Driver	18.98
W_{dri}	Width of Driver	3
D	Distance from Driver to Director	2.7
L_{dir}	Length of Director	15.9
W_{dir}	Width of Director	3
S_{dir}	Separation between each director	2.7

The return loss (S_{11}) measurement based on both CST simulation and measured data have been presented in Fig. 4. From simulation data, we can see that the center resonance frequency is at 3.40 GHz with broad bandwidth of 1.20 GHz starting from 3.12 GHz to 4.32 GHz. Within this range, the return loss value is less than -10 dB $(S_{11} < -10\ dB)$ and the maximum return loss value is -28 dB at the resonance frequency (blue line).

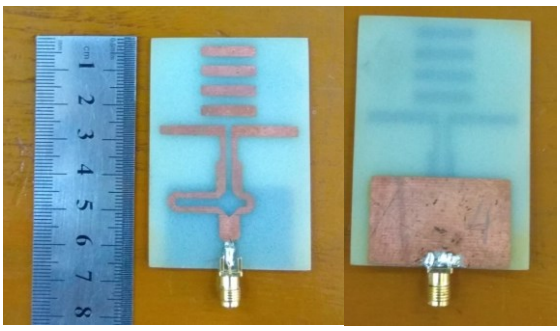

(a) (b)

Fig. 3. The fabricated antenna (a) front side and (b) the backside view

The measured value of the fabricated antenna shows similar trend and we found that -10 dB bandwidth starts from 3.04 GHz to 4.38 GHz with maximum return loss (S_{11}) value of -44.7 dB (red line). Thus, this antenna is usable for UWB applications as the bandwidth of the antenna $(\Delta f = 1.38\ GHz\ (experimental)\ or\ 1.20\ GHz\ (simulated))$ is much greater than 20% of center frequency $(\Delta f = f_c \times 20\% = 0.68 GHz)$ or 500 MHz recommended by FCC.

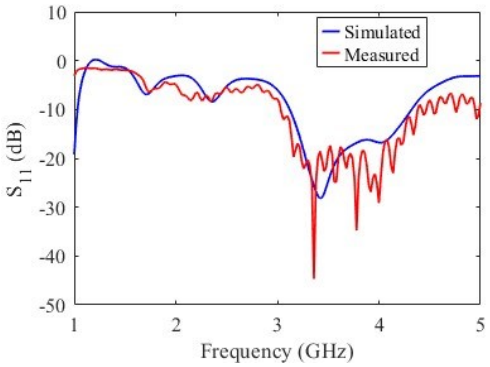

Fig. 4. Return loss graphs of both simulation (blue line) and experiment (red line) results of the antenna

It is desirable to have the Voltage Standing Wave Ration $(VSWR)$ value of any antenna to be less than 2 in its operating resonance frequency and within the bandwidth. The simulation and experiment data of our antenna is shown in the Fig. 5. The simulation result shows that the VSRW is less than 1.9 throughout the entire bandwidth (from 3.12 GHz to 4.32 GHz). Moreover, 90% of the bandwidth has a VSWR value even less than 1.4 and at the resonance frequency $(f_c = 3.4\ GHz)$ the VSWR is 1.08. However, the measured result shows that the antenna has VSWR value less than 1.4 within the entire bandwidth. At resonance frequency $(f_c = 3.36\ GHz)$, VSWR value is only of 1.18. These results confirms that the antenna is a perfect impedance match with that of the feedline connection.

The gain and the directivity of the antenna have been analyzed. Figure 6 shows the simulation result of the gain and directivity of the antenna for entire bandwidth. The gain and directivity of the antenna are found to be around 5 dB and 6 dB, respectively.

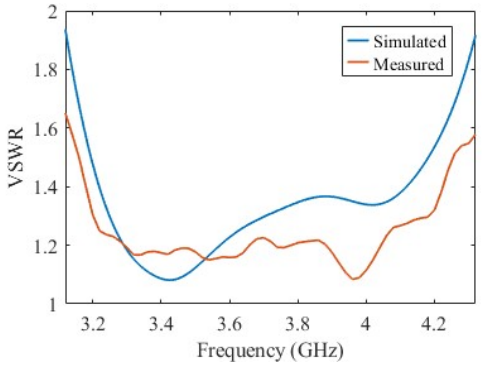

Fig. 5. VSWR vs frequency graph. Blue line shows the simulation result and red line gives the experiment result of the antenna.

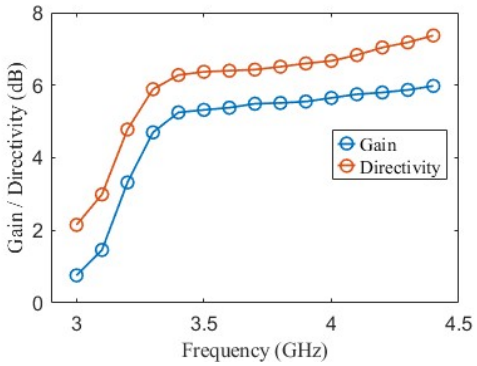

Fig. 6. Gain and directivity vs frequency graph (simulation result) of the antenna

In CST, we have simulated the farfield radiation gain and 3D radiaton pattern at resonance frequency $(f_c = 3.4\ GHz)$ as shown in the Fig. 7. It is found that the main lobe gain is 5.23 dB along the longitudinal direction of the antenna $(\theta = \varphi = 90^0)$ and half power radiation angle (angular width) is 78.5^0 and front to back ratio is 13.1 dB. Both gain and 3D radiation pattern shows a symmetric half-dumbbell shape radiation pattern at resonance frequency.

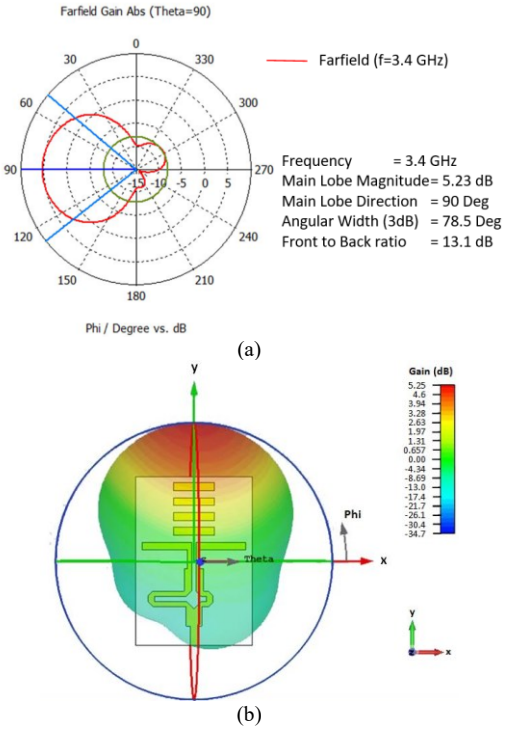

Fig. 7. (a) Farfiled radiation gain and (b) 3D radiation pattern at resonance frequency, $f_c = 3.4\ GHz$

The radiation pattern of the fabricated antenna with respect to the forward transmittance (S_{21}) has been measured using VNA as shown in Fig. 8. It is to be noted that both the resonance frequency and radiation pattern of the fabricated antenna differ slightly from that of simulation result. It is found that at practical resonance frequency $(f_c = 3.36\ GHz)$ the shape of the radiation pattern has some irregularities with main gain lobe at around 82^0. The measured gain value is 5.33 dB. However, the gain and directivity difference from that of simulation results may be due to lack of perfect measurement environment and instrument's calibration scaling mismatch.

We have analyzed the impedance of the antenna for a frequency range of 3.20 GHz to 3.40 GHz using Smith chart. The Smith chart data are from the VNA and presented in Fig. 9. It is found that at practical resonance frequency ($f_c = 3.36\,GHz$) the impedance of the antenna is $Z = 50.2 + j1.33\ \Omega$, which is very close to that of simulation impedance of 50 Ω. The summary of all the obtained simulation and experiment results are presented in Table II. Impact of number of directors and size of the truncated ground plane of the antenna have been analyzed using the CST studio software. From simulation results, it is confirmed that adding number of directors (one to four) in the design pattern, the antenna gain and directivity increases around 0.25 dB for each addition of directors.

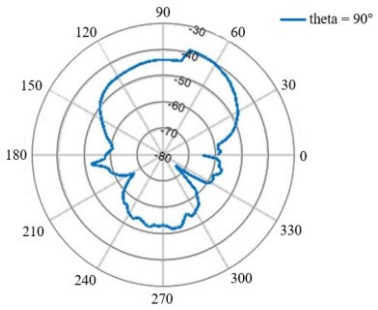

Fig. 8. Measured radiation pattern of the fabricated antenna

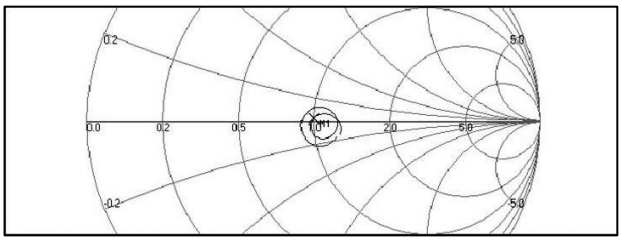

Fig. 9. Impedance measurement of the antenna for a frequency range of 3.2 GHz to 3.4 GHz using Smith chart

TABLE II
SUMMARY OF BOTH SIMULATION AND EXPERIMENT RESULT OF THE ANTENNA

Parameter	Simulated Value	Measured Value
Center frequency, f_c	3.4 GHz	3.36 GHz
Bandwidth	1.20 GHz	1.34 GHz
Lower cutoff frequency, (f_L)	3.12 GHz	3.04 GHz
Upper cutoff frequency, (f_H)	4.32 GHz	4.38 GHz
Bandwidth efficiency	35%	40%
Return Loss (S_{11})	-28 dB	-44 dB
Impedance (real part)	50.005 Ω	50.2 Ω
VSWR	1.08	1.15
Gain	5.25 dB	5.33 dB

The gain value changes from 4.52 dB up to 5.25 dB and the directivity changes from 5.52 dB to 6.28 dB, as we change the director number from 1 to 4, respectively. The overall bandwidth of the antenna also gets affected due to the change in director number. It increases from 1.08 GHz up to 1.2 GHz. It is obvious that to keep the size of the antenna small, we need to have minimum number of directors within the quasi-Yagi antenna. Table III summarizes the effects of the number of directors on bandwidth, gain and directivity of our proposed antenna. However, the farfield radiation pattern of the antenna (along longitudinal direction, ($\theta = \varphi = 90^0$)) does not have any significant change due to variation in the director's number as shown in Fig. 10.

TABLE III
EFFECTS OF DIRECTORS ON ANTENNA BANDWIDTH, GAIN AND DIRECTIVITY

Number of directors	Bandwidth (GHz)	Gain (dB)	Directivity (dB)
1	1.08	4.52	5.52
2	1.08	4.73	5.72
3	1.19	4.99	6.01
4	1.2	5.25	6.28

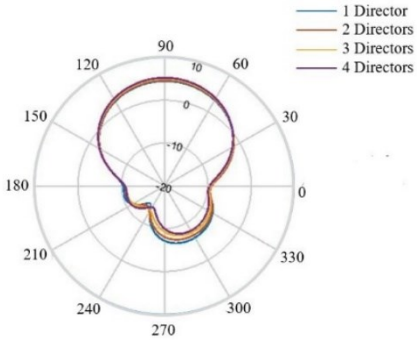

Fig. 10. Farfield radiation pattern ($\theta = \varphi = 90^0$) variation due to change in director numbers

For the size of truncated ground plane, we have simulated the plane for different longitudinal width size starting from 18 mm up to 26 mm, while keeping the number of directors as four. Table IV summarizes the obtain antenna parameters. The width size variation has huge impact of bandwidth and resonance frequency values of the antenna. The bandwidth (Δf) of the antenna increases (0.78 GHz up to 1.27 GHz) with increment in width size and the resonance frequency (f_c) shifts downward from 4.53 GHz to 3.40 GHz while width length (W_g) changes from 18 mm to 26 nm, respectively. However, the return loss (S_{11}) value at resonance frequency; lower and upper cutoff frequencies of the bandwidth changes arbitrarily. Figure 11 shows the return loss vs frequency graph depending on the change in ground plane width of the antenna.

Thus from the simulation result, we have chosen the number of directors to be four and the width of the ground plane of 23.9 mm within our fabricated antenna as both the values give favorable and significant results in antenna parameters. This antenna can be used for UWB applications such as radio frequency identification devices (RFID), radar, location tracking and sensor networks. More precisely, due to its favorable bandwidth of 1.34 GHz with resonance frequency of 3.36 GHz, it can be used for WiMAX and Fixed Wireless Access communication system operating in the 3.3 to 3.6 GHz band.

TABLE IV
CHANGE IN ANTENNA PARAMETERS DUE TO GROUND PLANE WIDTH (W_g) VARIATION.

Width, (W_g) (mm)	Lower cut-off freq., (f_L) (GHz)	Upper cut-off freq., (f_H) (GHz)	Bandwidth, (Δf) (GHz)	Resonating Freq., (f_c) (GHz)	Return Loss, (S_{11}) (dB)
18	4.00	4.78	0.78	4.53	-25
20	3.66	4.62	0.96	4.37	-42
22	3.36	4.44	1.08	4.17	-28
24	3.12	4.32	1.20	3.42	-28
26	2.89	4.16	1.27	3.40	-16

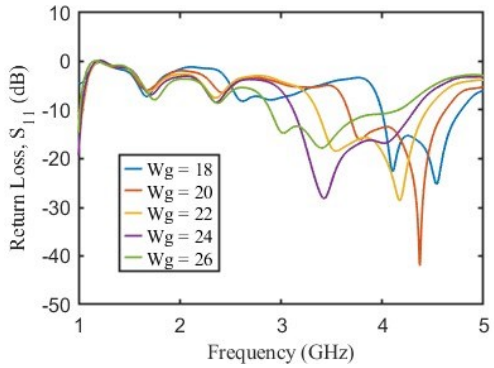

Fig. 11. Effect of ground plane width (W_g) on return loss (S_{11}) of the antenna

CONCLUSION

Our developed quasi-Yagi microstrip patch antenna has overcome the limitation of narrow-band effectively as well as provides the high directivity of the traditional Yagi-Uda antenna. The impact of increasing director numbers and optimizing the truncated ground plane as reflector have been studied. All the simulation works carried out in CST studio with rigorous optimization and the performance of a fabricated antenna has been verified with Vector Network Analyzer and Wave and Antenna Training System. Both the (simulation) and measured results have shown excellent agreement providing an ultra-wide bandwidth of (1.20 GHz) 1.34 GHz with lower and upper cutoff frequencies at (3.12 GHz) 3.04 GHz and (4.32 GHz) 4.38 GHz, respectively. The antenna gain of (5.32 dB) 5.33 dB and return loss of only (-28 dB) -44 dB were achieved at resonance frequency of (3.40 GHz) 3.36 GHz. Our designed and fabricated antenna has a compact size of 65 mm x 45 mm. For excellent half dumbbell shaped radiation pattern, this antenna may be used in various UWB applications such as RFID, radar, location tracking and sensor networks along with communication systems of upper S-band, like WiMAX and Fixed Wireless Access systems.

IV. ACKNOWLEDGEMENT

This research work has been carried out at Microwave and Optical Fiber Communication Laboratory of the Department of Electrical and Electronic Engineering, University of Dhaka, Bangladesh. This work has supported by Higher Education Quality Enhancement Project (HEQEP) program of University Grants Commission of Bangladesh (UGC). Authors would like to thank technical persons of Central Science Workshop, University of Dhaka, Bangladesh for their support.

REFERENCES

[1] H. Yagi, "Beam transmission of ultra short waves," *Proc. Inst. Radio Eng.*, vol. 16, no. 6, pp. 715–740, 1928, https://doi.org/10.1109/JRPROC.1928.221464

[2] S. UDA, "On the WireleSS Beam Of Short Electric Waves. (I)," *J. Inst. Electr. Eng. Japan*, vol. 46, no. 452, pp. 273–282, 1926

[3] J. Huang and A. C. Densmore, "Microstrip yagi array antenna for mobile satellite vehicle application," *IEEE Trans. Antennas Propag.*, vol. 39, no. 7, pp. 1024–1030, 1991, https://doi.org/10.1109/8.86924

[4] Y. Qian, W. R. Deal, N. Kaneda, and T. Itoh, "Microstrip-fed quasi-Yagi antenna with broadband characteristics," *Electron. Lett.*, vol. 34, no. 23, pp. 2194–2196, Nov. 1998, https://doi.org/10.1049/EL:19981583

[5] "Federal Communications Commission: 'Revision of Part 15 of the Commission's Rules Regarding Ultra-wideband Transmission Systems'. First Report and Order, FCC 02.V48, Apr. 2002.

[6] K. S. Ryu and A. A. Kishk, "UWB antenna with single or dual band-notches for lower WLAN band and upper WLAN band," *IEEE Trans. Antennas Propag.*, vol. 57, no. 12, pp. 3942–3950, Dec. 2009, https://doi.org/10.1109/TAP.2009.2027727

[7] S. Nikolaou, N. D. Kingsley, G. E. Ponchak, J. Papapolymerou, and M. M. Tentzeris, "UWB elliptical monopoles with a reconfigurable band notch using MEMS switches actuated without bias lines," *IEEE Trans. Antennas Propag.*, vol. 57, no. 8, pp. 2242–2251, 2009, https://doi.org/10.1109/TAP.2009.2024450

[8] M. Ojaroudi, C. Ghobadi, and J. Nourinia, "Small square monopole antenna with inverted T-shaped notch in the ground plane for UWB application," *IEEE Antennas Wirel. Propag. Lett.*, vol. 8, pp. 728–731, 2009, https://doi.org/10.1109/LAWP.2009.2025972

[9] K. Quzwain, A. Ismail, and A. Sali, "Compact High Gain and Wideband Octagon Microstrip Yagi Antenna," vol. 36, no. 8, pp. 524–533, Nov. 2016, http://dx.doi.org/10.1080/02726343.2016.1236060

[10] Z. Hu, Z. Shen, W. Wu, and J. Lu, "Low-Profile Top-Hat Monopole Yagi Antenna for End-Fire Radiation," *IEEE Trans. Antennas Propag.*, vol. 63, no. 7, pp. 2851–2857, Jul. 2015, https://doi.org/10.1109/TAP.2015.2427853

[11] K. Jiang, Q. G. Guo, and K. M. Huang, "Design of a wideband quasi-Yagi microstrip antenna with bowtie active elements," *2010 Int. Conf. Microw. Millim. Wave Technol. ICMMT 2010*, pp. 1122–1124, 2010, https://doi.org/10.1109/ICMMT.2010.5525084

[12] Y. Liu, H. Liu, M. Wei, and S. Gong, "A novel slot Yagi-like multilayered antenna with high gain and large bandwidth," *IEEE Antennas Wirel. Propag. Lett.*, vol. 13, pp. 790–793, 2014, https://doi.org/10.1109/LAWP.2014.2318313

[13] Y. Ding, Y. C. Jiao, P. Fei, B. Li, and Q. T. Zhang, "Design of a multiband Quasi-Yagi-type antenna with CPW-to-CPS transition," *IEEE Antennas Wirel. Propag. Lett.*, vol. 10, pp. 1120–1123, 2011, https://doi.org/10.1109/LAWP.2011.2170950

[14] Y. Qian and T. Itoh, "Broadband uniplanar microstrip-to-CPS transition," *Asia-Pacific Microw. Conf. Proceedings, APMC*, vol. 2, pp. 609–612, 1997, https://doi.org/10.1109/APMC.1997.654615

[15] H. D. Lu, L. M. Si, and Y. Liu, "Compact planar microstrip-fed quasi-Yagi antenna," *Electron. Lett.*, vol. 48, no. 3, pp. 140–141, Feb. 2012, https://doi.org/10.1049/EL.2011.3458/CITE/REFWORKS

[16] H. K. Kan, R. B. Waterhouse, A. M. Abbosh, and M. E. Bialkowski, "Simple broadband planar CPW-fed quasi-Yagi antenna," *IEEE Antennas Wirel. Propag. Lett.*, vol. 6, pp. 18–20, 2007, https://doi.org/10.1109/LAWP.2006.890751

[17] K. Han, Y. Park, H. Choo, and I. Park, "Broadband CPS-fed Yagi-Uda antenna," *Electron. Lett.*, vol. 45, no. 24, pp. 1207–1209, 2009, https://doi.org/10.1049/EL.2009.1330/CITE/REFWORKS

[18] J. R. Aguilar, M. Beadle, P. T. Thompson, and M. W. Shelley, "The microwave and RF characteristics of FR4 substrates," *IEE Colloq.*, no.

206, 1998, https://doi.org/10.1049/IC:19980078

[19] C. Balanis, *Antenna Theory: Analysis and Design*. 2005.

[20] R. J. P. Douville and D. S. James, "Experimental Study of Symmetric Microstrip Bends and Their Compensation," *IEEE Trans. Microw. Theory Tech.*, vol. 26, no. 3, pp. 175–182, 1978, https://doi.org/10.1109/TMTT.1978.1129340

[21] W. Nannan, Q. Jinghui, L. Shu, D. Weibo, and W. Wei, "Research on wide beamwidth and high gain quasi-Yagi antenna," *ISAPE 2008 - 8th Int. Symp. Antennas, Propag. EM Theory Proc.*, pp. 302–305, 2008, https://doi.org/10.1109/ISAPE.2008.4735204

[22] N. Kaneda, W. R. Deal, Y. Qian, R. Waterhouse, and T. Itoh, "A broad-band planar quasi-Yagi antenna," *IEEE Trans. Antennas Propag.*, vol. 50, no. 8, pp. 1158–1160, Aug. 2002, https://doi.org/10.1109/TAP.2002.801299